Motor control of sound frequency in birdsong involves the interaction between air sac pressure and labial tension

Rodrigo Alonso,[1,*] Franz Goller,[2] and Gabriel B. Mindlin[1]

[1]*Department of Physics, FCEyN, University of Buenos Aires, Ciudad Universitaria, Pab I, cp 1428, Buenos Aires, Argentina*

[2]*Department of Biology, University of Utah, Salt Lake City, Utah 84112, USA*

(Received 23 August 2013; revised manuscript received 23 December 2013; published 10 March 2014)

Frequency modulation is a salient acoustic feature of birdsong. Its control is usually attributed to the activity of syringeal muscles, which affect the tension of the labia responsible for sound production. We use experimental and theoretical tools to test the hypothesis that for birds producing tonal sounds such as domestic canaries (*Serinus canaria*), frequency modulation is determined by both the syringeal tension and the air sac pressure. For different models, we describe the structure of the isofrequency curves, which are sets of parameters leading to sounds presenting the same fundamental frequencies. We show how their shapes determine the relative roles of syringeal tension and air sac pressure in frequency modulation. Finally, we report experiments that allow us to unveil the features of the isofrequency curves.

DOI: 10.1103/PhysRevE.89.032706 PACS number(s): 87.19.−j, 05.45.−a

I. INTRODUCTION

Motor control of complex behaviors requires integration of muscle-generated movements with the biomechanical properties of effector organs to achieve the desired behavioral output [1–3]. Effector organs frequently introduce nonlinearities, which give rise to complex relationships between different coordinated muscle systems and biomechanics. These relationships generate a highly complex multivariate parameter space from which control strategies for a behavioral output must be selected. At the same time, the nonlinear relationships introduce the need for high precision, because small variation in motor instructions can cause large variability in the behavioral output.

Investigation of how the brain selects motor control strategies and whether or not the selection depends on the context of motor sequences in which it is embedded requires a comprehensive understanding of the complex parameter space at the level of the target organs for motor control. Production of voiced sounds, such as in human speech and birdsong, is an example for such a highly complex motor control task for which spatially separated motor systems must directly and indirectly control multiple nonlinear biomechanical relationships in the effector organs. Sound production involves respiratory control for generating airflow, control of the vocal organ to position the vibrating tissues and regulate their tension, as well as control of upper vocal tract structures to adjust filter properties. Precise motor control is required for generating specific acoustic features, and their stereotyped production is critical for effective communication [4].

One such acoustic feature is sound frequency, which is determined by the oscillation rate of the sound generating tissue (e.g., vocal folds in mammals, labia in songbirds). The rate of tissue oscillation depends on four main physiological parameters: the viscoelastic properties of the vibrating tissue, the aerodynamic forces (i.e., pressure), direct control of tension through muscle activity, and source-filter interactions. These different variables influence sound frequency to varying degrees and encompass nonlinearities, thus creating a complex parameter space for its neural control [5,6].

Song development in songbirds occurs during a limited period for sensorimotor refinement, at the end of which the song becomes highly stereotyped. In canaries (*Serinus canaria*), the song is composed of a series of different trills, each of which consists of a repeated syllable type. Most syllables are frequency modulated (up- or down-sweeps) and fall within a frequency range between 2 and 7 kHz. This song organization offers the opportunity to investigate how the same frequency is controlled in the different contexts of different syllables. Because sound frequency is dependent on a complex interplay between the neural control of different motor systems and the nonlinear biomechanical effects of syringeal morphology and aerodynamic effects on the vibrating tissues, the answer to this question will offer insight into the general issue of whether or not motor control strategies make use of the complex landscape of parameters. Here we address this question by first theoretically exploring the parameter space for frequency control to predict control strategies and then testing these predictions with experimental data.

II. PHYSIOLOGY OF BIRDSONG PRODUCTION

The avian vocal organ is the syrinx, which is located at the juncture between the bronchi and the trachea. Studies of subsyringeal air sac pressure, bilateral airflow, and the EMG activity of several syringeal muscles revealed a general pattern of vocal control [6–8], but many details, including differences between species, are still unknown [6]. For example, a strong correlation between the EMG activity of the ventral syringeal muscle (vS) (the largest syringeal muscle) and the fundamental frequency of the vocalization exists in brown thrashers, but the relationship is very different in zebra finches [6,7]. Syringeal muscles are also involved in the gating of the vocalizations. The activity of the ventral tracheobronchial muscle (vTB) is correlated with an active opening of the syringeal lumen (abduction) that would help to stop the vocalizations, allowing brief inspirations in between syllables. Activity in the dorsal tracheobronchial muscle (dTB) causes adduction of the syrinx [7–9]. Thus, vocal control involves delicately orchestrated syringeal motor gestures and large expiratory events that establish airflow between the labia at the syrinx. At the right phonatory position, labial oscillations are induced, and it is

*Corresponding author: ralonso@df.uba.ar

these modulations of the airflow that constitute the origin of sound. In this paradigm, the modulation of the fundamental frequency of the vocalizations is caused by varying the tension of the oscillating labia. Tension can be actively controlled by syringeal muscles. Additional support for this mechanism comes from simulations of simple computational models describing the biomechanics of the labial oscillations. Using recorded EMG activity from vS muscles as time-dependent parameters representing the elastic restitution of the labia, synthetic sounds could be generated with frequency modulations qualitatively similar to those in the recorded song [10].

Interestingly, the study of the suboscine Great Kiskadee (*Pitangus sulfuratus*) provided a clear example of an alternative mechanism of frequency control in birdsong production. In that species, the modulations of the fundamental frequency were highly correlated to air sac pressure. Moreover, after denervation of the syringeal muscles, the strong correlation between fundamental frequency and air sac pressure patterns remained unchanged. In this species, a nonlinear restitution force for the oscillating membrane folds was found to be essential to reproduce the frequency modulations of the observed vocalizations [11]. This surprising lack of frequency control by syringeal muscles in Kiskadees is in strong contrast to songbirds (e.g., [6,12,13]), and, thus, posed the general question of to what degree air sac pressure contributes to the regulation of sound frequency.

Song production in the zebra finch (*Taeniopygia guttata*) constitutes another example for how air sac pressure contributes to frequency control. The song of this species consists of many syllables that are spectrally very rich (i.e., sounds that are made up of many equally spaced harmonics) interspersed with a few tonal elements. Moreover, there is a very precise relationship between the harmonic content and fundamental frequency of the uttered sounds; low-frequency sounds are harmonically very rich, while the higher-frequency sounds are more tonal. This relationship was investigated in many syllables uttered by different birds, and the functional form relating those acoustic features was the same for all of them [13,14]. Remarkably, it is precisely what can be expected if a periodic signal is born in a saddle node in a limit cycle bifurcation [15]. In this mechanism, when the periodic oscillation is born, the phase space is left with the ghost of the two fixed points that were annihilated in the bifurcation, which slows down the passing trajectory. According to this paradigm, the frequency of the labial oscillations is very sensitive to how much air sac pressure (control parameter) deviates from the value at which the bifurcation takes place.

In both examples, nonlinear effects are needed to account for the role of air sac pressure in modulating the phonation frequency. If the labial motion could be described in terms of a linear oscillation, the restitution constant of the tissue would be the only factor determining the frequency of the oscillations. But nonlinear effects are unavoidable in a description of labial motion: even the bounding of the labial motion requires a nonlinear dissipation. This raises the question of how nonlinearities link the respective contributions of muscle activity and air sac pressure in the process of determining the frequency of the labial oscillations. To explore this issue, we investigated a simple model for labial oscillation that includes nonlinearities in the dissipation and in the restitution. By means of both analytical and numerical work, we explored how muscle activity and air sac pressure synergistically contribute to frequency modulation.

III. A MODEL FOR BIRDSONG PRODUCTION

We explore the dynamics of a physical model for a syringeal labium, where different forces drive a unitary mass representing the labium [10,14,16–18,20,21]. The forces are (i) the elastic restitution, which depends on the displacement of the labium from its equilibrium position, (ii) the linear dissipation (proportional to the labial velocity), which includes a negative contribution accounting for the transfer of energy from the airflow to the mass as a mucosal wave propagates along the labium, (iii) the nonlinear dissipation, which is responsible for bounding the oscillations and represents either labia collapsing against containing walls or against each other, and (iv) forces representing active adduction and abduction. The model reads

$$\frac{dx}{dt} = y,$$
$$\frac{dy}{dt} = -\kappa(t)\gamma^2(x+\epsilon x^3) + [\beta(t)-\beta_0]\gamma y - cx^2\gamma y + \gamma^2 f_{\mathrm{add}}(t) - \gamma^2 f_{\mathrm{abd}}(t).$$

In this set of equations, x stands for the midposition of a labium, $\kappa(t)$ for the elastic restitution coefficient, and $\beta(t)-\beta_0$ for the negative dissipation coefficient. The model includes a cubic term in the restitution (ϵx^3), a nonlinear dissipation term (cx^2y), and two forces independent of either x or dx/dt: the adducting force (f_{add}) and the abducting force (f_{abd}). The coefficient γ is a time scaling factor. In this model, there are two well-separated time scales. The parameters $\kappa(t)$ and $\beta(t)-\beta_0$ fluctuate in the time scales of the syllables (in the order of 100 ms), while $x = x(t)$ will present oscillations with frequencies in the kHz range.

The analysis of the linear part of the previous model allows integrating the experimental results mentioned in the Introduction. The negative dissipation term provided by the airflow to the labia is proportional to the subsyringeal pressure [21] and has to overcome a threshold for oscillations to start. On the other hand, increasing the value of the elastic restitution increases the frequency of the oscillations. Since the elastic restitution will depend on the tension of the oscillating labia, and those are stretched as the ventral syringeal muscle is contracted, one is inclined to think of its activity as an analog control of the vocalization frequency, just as the level of the air sac pressure can be thought of as a digital on-off switch for the vocalization onset.

Nonlinearities, on the other hand, are unavoidable in an operational model for birdsong production. Once the equilibrium position loses stability, labial oscillations are bounded. The lateral and medial labia might collide with each other or with their containing walls, losing energy, as the departure of the equilibrium position is large enough. The nonlinear dissipation term in our model is the lowest-order term capable of describing that effect [21,22]. There are other nonlinearities that can play a role in the functioning of the syrinx. In the model presented above, a nonlinear term for the restitution is

considered. Restitution is to be modeled as an odd function of the variable describing the departing of the oscillating body from equilibrium. Therefore, we include nonlinear terms in the restitution up to the same order used to account for the saturation of the oscillations.

Once that nonlinearity is included in our model, it is not possible to separate the roles of the air sac pressure and the tension in the determination of the fundamental frequency of phonation. Both participate synergistically in order to achieve a given acoustic feature.

IV. ISOFREQUENCY CURVES

To unveil how tension κ and pressure β participate in the determination of the frequency, we plotted isofrequency curves: curves in the parameter space (κ,β) such that the model, integrated for parameters in the curve, led to oscillations of a given frequency. Starting with the case $\epsilon = 0$, $c = 1$, it is possible to find a regime in which the isofrequencies can be computed analytically. If neither the active adduction nor abduction are present, our model can be written as

$$\frac{d^2x}{dt} + \kappa\gamma^2 x - \beta\gamma\frac{dx}{dt} + \gamma x^2\frac{dx}{dt} = 0. \tag{1}$$

For $\beta\gamma \gg 1$ and $\kappa\gamma/\beta \ll 1$, the equation describes a relaxation oscillation dynamics. Writing $v = \frac{dx}{dt} + \beta\gamma(\frac{x^3}{\epsilon\beta} - x)$, the system above reads

$$\frac{dx}{dt} = \beta\gamma\left[\frac{v}{\beta\gamma} - \left(\frac{x^3}{3\beta} - x\right)\right], \tag{2}$$

$$\frac{d}{dt}\left(\frac{v}{\beta\gamma}\right) = -\frac{\kappa\gamma}{\beta}x. \tag{3}$$

Defining $V \equiv v/(\beta\gamma)$, the dynamics of the system is determined by the structure of the null cline $V = (\frac{x^3}{3\beta} - x)$. Any initial condition (except the origin) will rapidly converge, almost horizontally onto the null cline. Then, it will slowly crawl close to the null cline until it reaches one of its two knees, to rapidly jump to the other branch of the cubic null cline. Neglecting the times necessary for the jumps, the period of oscillation can be approximated as twice the time the system crawls close to either of the branches, which leads to an approximation of the period of the oscillations [15],

$$T = \frac{\beta}{\kappa\gamma}(3 - 2\ln 2), \tag{4}$$

or that the frequency of the oscillation is $\varpi \approx \frac{\kappa}{\beta}$.

In other words, within the range of applicability of the derivation, the isofrequency curves in the (β, κ) space are straight lines with positive slope. Notice that in this way, the gesture pressure and tension necessary for achieving a given acoustic feature need to be coordinated in a precise manner. For example, a syllable of constant fundamental frequency that is uttered while the pressure decreases will need a labial tension that decreases accordingly in order for the vocal device to operate within an isofrequency curve.

The above analysis is valid for high values of pressure, since the separation of slow and fast time scales requires that $\kappa\gamma/\beta \ll 1$. The limit of low-pressure values, which are important for understanding the behavior of the system close to the bifurcations, requires a different approach. For a dynamical system close to bifurcation, it is possible to perform a series of changes of variables, which eliminate all the nonresonant terms. This procedure is called normal form reduction.

For the dynamical system (1), we can perform a scaling of the time $t = \Gamma\tau$, with $\Gamma = 1/(\gamma\sqrt{\kappa})$, leading to

$$\begin{aligned}\frac{dx}{d\tau} &= y,\\ \frac{dy}{d\tau} &= -(x + \epsilon x^3) + \frac{\beta}{\sqrt{\kappa}}y - \frac{1}{\sqrt{\kappa}}x^2 y.\end{aligned} \tag{5}$$

Defining the following new complex variables (z,$z*$) by

$$\begin{pmatrix}x\\ y\end{pmatrix} = \begin{pmatrix}1 & 1\\ i & -i\end{pmatrix}\begin{pmatrix}z\\ z^*\end{pmatrix}, \tag{6}$$

we can perform a change of variables, and keep only the resonant terms, which leads to

$$\frac{dz}{d\tau} = \left(\frac{\beta}{\sqrt{\kappa}} + i\right)z + \left(\frac{3}{2}\epsilon i - \frac{1}{2\sqrt{\kappa}}\right)z|z^2|, \tag{7}$$

which in terms of the modulus and phase reads as follows:

$$\begin{aligned}\frac{d\rho}{dt} &= \gamma\beta\rho - \frac{1}{2}\gamma\rho^3,\\ \frac{d\phi}{dt} &= \gamma\sqrt{\kappa}\left(1 + \frac{3}{2}\epsilon\rho^2\right).\end{aligned} \tag{8}$$

This allows us to describe the isofrequency curves. Oscillatory dynamics occurs as $\rho^2 = \beta$, and therefore for a given value of the frequency w, the corresponding isofrequency will read

$$w = \gamma\sqrt{\kappa}(1 + 3\epsilon\beta).$$

This implies that close to the bifurcation at which the oscillations start, in the (β,κ) space, the isofrequencies start with negative slope as long as $\epsilon \neq 0$; the larger the frequency value, the larger the slope in absolute value.

The two regimes discussed above are qualitatively different. In the first case, the slopes of the isofrequency curves are positive, while in the second case, the slopes are negative. This change in slope requires important differences in motor control. For example, if the tension is kept constant during phonation, in the first case the frequency of the vocalizations will decrease as the pressure increases. In the second case, the fundamental frequency of the vocalizations will be positively correlated with the pressure. The different nonlinearities present in the system are responsible for different effects at different regions of the parameter space, and the bird has to delicately coordinate the motor instructions to achieve a given acoustical feature.

V. DESCRIBING THE ISOFREQUENCIES

As we described in the Introduction, a nonlinearity that is present in every model of phonation is a dissipative one capable of bounding the labial oscillations. On the other hand, a model for suboscine phonation required a nonlinear restitution to account for the correlation between fundamental frequency and pressure, even under a nerve cut that implied that no

modulation could be attributed to syringeal muscle activity [11]. A nonlinear restitution was also included in the modeling of zebra finch vocalizations. In that case, it was a requirement for having a saddle node in limit cycle bifurcations, which were used to explain the relationship that exists between the spectral content and fundamental frequency [13]. Yet it is not known whether this nonlinearity is present in other species presenting more tonal sounds.

To unveil the nature of the isofrequencies structuring the parameter space of a model for phonation, we explored the variations present in the acoustic features of repeating syllables. Many species sing songs that consist of repeated elements. A paradigmatic example is the domestic canary (*Seriuns canaria*), whose song consists of a series of different syllables that are repeated and grouped in sets that constitute phrases. During the repetition of a syllable, the bird repeats the same syllable in a stereotyped manner, but with small variations in the physiological instructions. Assuming that the variations of different instructions are uncorrelated, we can use them to unveil the organization of the isofrequency curves by exploring areas of the parameter space around specific values. The generation of song with repeating syllables implies changing periodically the parameters of the model. Yet the map of isofrequency curves is a useful tool for understanding the dynamics of the problem since the labial oscillations are in the order of kHz, while the parameter modulation occurs at most in the order of 30 Hz [18,19].

The diversity of syllables present in canary song is characterized by a variety of frequency modulations (up-sweeps, down-sweeps, constant frequency sounds, etc.). It was proposed that such diversity could be generated by different phase differences between the air sac pressure and the labial tension during phonation [18]. In Fig. 1, we illustrate three sets of trajectories in the parameter space. Each set is composed of six subsets of 19 trajectories. Each subset assumes an average phase difference between the tension and the pressure (i.e., an elliptical trajectory in the parameter space), and the 19 trajectories of the subset are generated as noise is added to the pressure and the tension components of the basic ellipse.

We generated synthetic syllables with each of the trajectories in the parameter space. We then identified, for each syllable, the time at which the parameter β (representing the air sac pressure) reached its maximum and inspected the spectral properties of the sound segment of 1024 points around a chosen time to record its fundamental frequency. Due to the introduced noise, the maxima of the pressure will be different for different trajectories within a subset. That (together with the fluctuations of the tension) simulates the biological variation of physiological parameters in the process of repeating a syllable type. Under the hypothesis that the fluctuations of the tension are random, plotting the frequency of the segments as a function of the maximum pressure reflects the nature of the isofrequencies. In a region of the parameter space where the isofrequencies present a negative slope in the (β,κ) space, the correlation between frequency and pressure should be positive, since larger explorations in the pressure will intersect isofrequencies corresponding to larger values. Similarly, in a region of the phase space presenting isofrequencies of positive slope, the correlation between frequency and pressure should be negative.

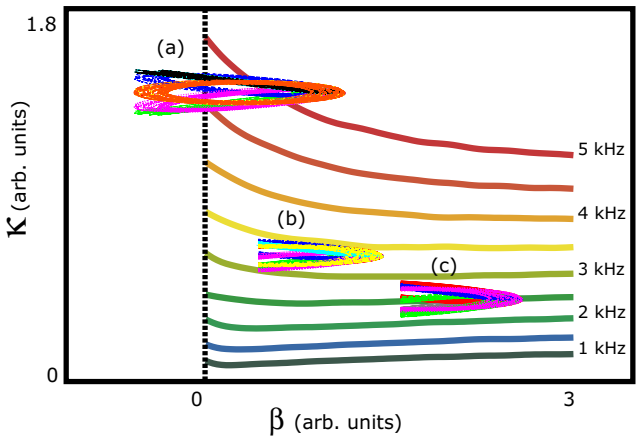

FIG. 1. (Color online) Isofrequency curves in the parameter space (β,κ) together with three sets of trajectories used to synthesize syllables. Notice that each set pierces into qualitatively different regions of the parameter space where the isofrequencies have negative, zero, or positive slopes. The isofrequencies and trajectories were computed using the model introduced previously (see Sec. III) with $\epsilon = 0.3$ and $c = 2$. For every set we generate six different paths with 19 repetitions apiece which lead to the same $\beta_{\max}$ and $\kappa_{\max}$. Each path is generated using periodic functions with a phase difference between $\beta(t)$ and $\kappa(t)$ of 0, $-\pi/4$, $-\pi/2$, $\pi/2$, π, and $3/4\pi$, respectively. Within each path, random fluctuations (up to 20% of their amplitude) were added to $\beta(t)$ and $\kappa(t)$. To produce synthetic syllables with large β values such as sets (b) and (c), we added a periodic *step* function of $f_{\text{add}} = 1.0$ for values of β below 0.6 and 1.8, respectively. This parameter represents the action of muscles involved in active gating, which prevent phonation by adducting the labia. Trajectory parameters: (a) $\beta = 0.3 + 0.7\cos(20\pi)$, $\kappa = \kappa_{0a} + 0.05\cos(20\pi + \theta)$; (b) $\beta = 0.6 + 0.7\cos(20\pi)$, $\kappa = \kappa_{0b} + 0.05\cos(20\pi + \theta)$; (c) $\beta = 1.8 + 0.7\cos(20\pi)$, $\kappa = \kappa_{0c} + 0.05\cos(20\pi + \theta)$. κ_{0a}, κ_{0b}, and κ_{0c} are slightly different within subsets to reach the same $\beta_{\max}$,$\kappa_{\max}$.

In Fig. 2, we display the frequencies as a function of the maximum pressure for the three sets of trajectories displayed in Fig. 1. For each set, the six subsets were analyzed independently. We found that the slopes obtained as the 19 pairs (frequency, maximum pressure) of each of the six subsets were linearly fitted presented little variation (see the figure caption for details). This means that regardless of the average time evolution of the tension, the slopes were determined by the structure of the isofrequencies.

We tested this paradigm by recording sound and air sac pressure from canaries. The recording setup consisted of a microphone (TAK-STAR SGC 568) placed in front of each cage. Sound was recorded using a microphone preamplifier (PR4V SM pro audio) and a multichannel sound card (MAYA 1010, 44.1 kHz sample rate) directly onto a computer. Air sac pressure was monitored through a flexible cannula (Silastic tubing, o.d. 1.65 mm), which was inserted through the abdominal wall into the anterior thoracic air sac under Ketamine/Xylazine anesthesia. The free end of the cannula was connected to a miniature piezoresistive pressure transducer (Fujikura model FPM-02PG), which was mounted on the bird's back, following methods described in detail [7,8].

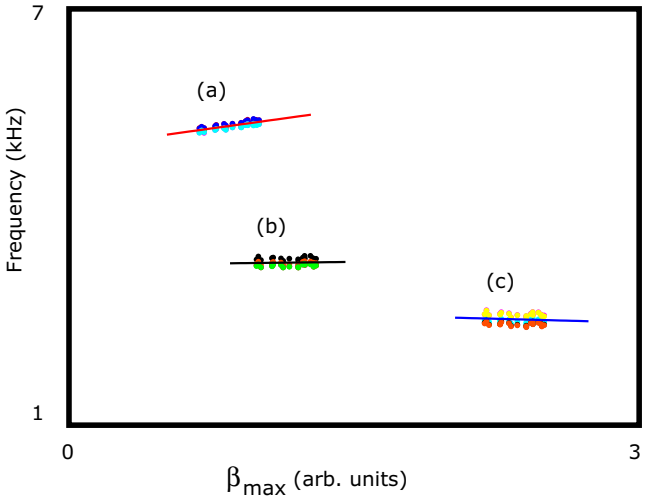

FIG. 2. (Color online) Theoretical results. Fundamental frequency vs $\beta_{\max}$ from three sets of trajectories displayed in Fig. 1. Linear regressions: (a) $f(x) = 379.03x + 4992.66$, $\sigma = 47.781$; (b) $g(x) = 27.61x + 3310.85$, $\sigma = 43.24$; (c) $h(x) = -69.79x + 2586.43$, $\sigma = 62.55$.

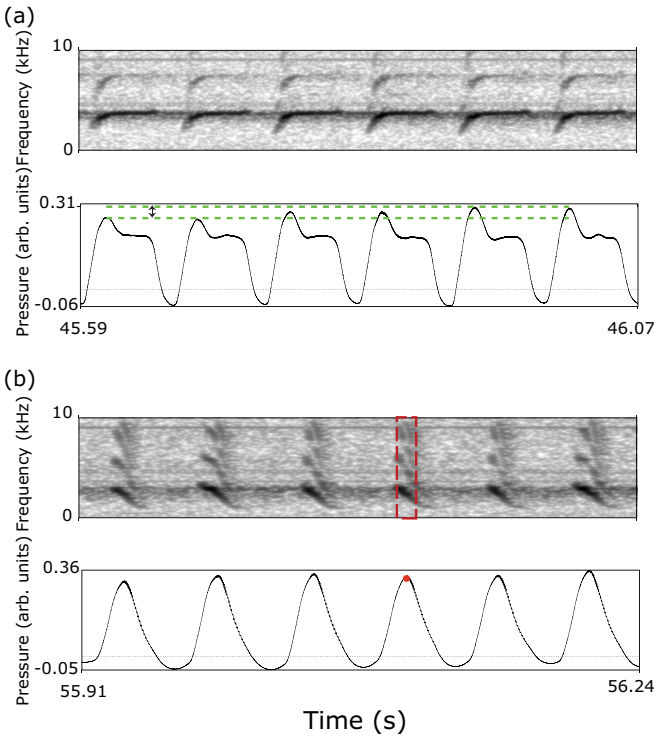

FIG. 3. (Color online) Two examples of experimental data from simultaneous recordings of air sac pressure and song in a domestic canary (*Serinus canaria*). (a) (First panel) Sonogram from *up-sweep* syllable. (Second panel) Air-sac pressure of the uttered vocalization. Green lines highlight the natural fluctuations of pressure maxima. (b) Schematic representation of experimental methods. (Third panel) Sonogram for a *down-sweep* syllable. (Fourth panel) Air-sac pressure. The red dot indicates one pressure maximum; the red box represents the temporal window from which the fundamental frequency was computed (1024 points around the chosen time, for song and air sac pressure sampled at 44.1 kHz).

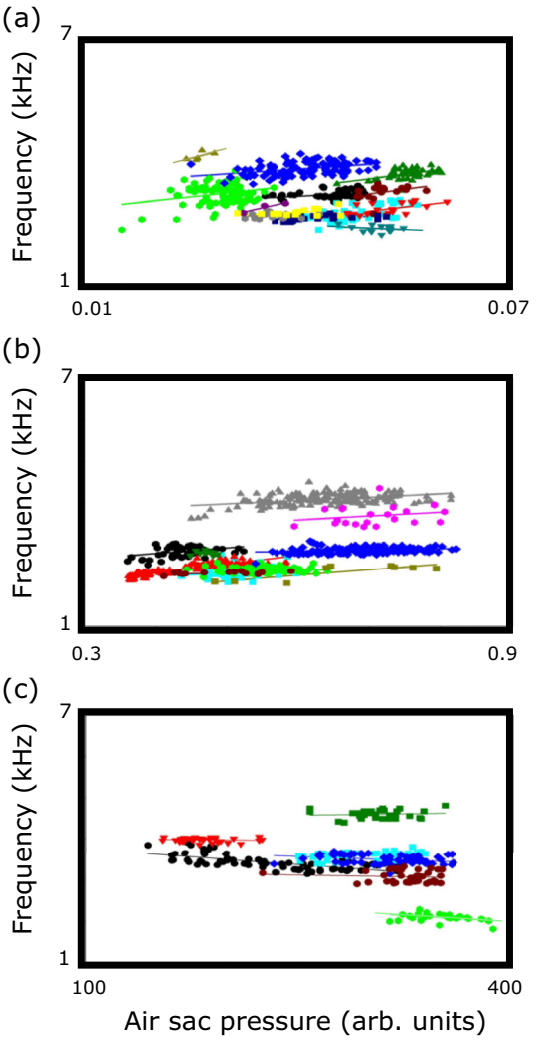

FIG. 4. (Color online) Experimental results. Pressure maxima vs fundamental frequency. (a) Bird 1, (b) bird 2, and (c) bird 3. Statistical parameters are displayed in Table I.

The voltage signal from the transducer was amplified and modulated to make it suitable for recording with a sound card (MAYA 1010).

Once we got simultaneous recordings of pressure and song for a bird, we selected repeated syllables within phrases that presented a constant number of pressure maxima. The reason for restricting our analysis to these patterns is that pressure patterns in canaries present a richer structure than a simple harmonic oscillation. In fact, it has been shown that they possess the same topological features as those of a driven nonlinear system [23,24]. Therefore, in some cases the variability can be translated into the disappearance of a maximum in the pressure gesture. By requiring the number of maxima in a pressure pattern to remain constant, we ascertain that we are exploring the vicinity of a specific region of the parameter space. In Fig. 3, we summarize the experimental methods revealing the isofrequency curves.

In Fig. 4, we show the results from three canaries. For each bird, we have used pressure and sound recordings of the complete syllabic repertoire, recorded on the same day.

TABLE I. Linear regression of experimental data.

Bird 1	Syllable	Color and Symbol	Slope	Significance	R^2	n
	1	Black circle	9140	0.0086	0.14	49
	2	Cyan square	25094	<0.0001	0.35	61
	3	Red triangle	19021	0.0003	0.44	25
	4	Light green hexagon	19553	0.0065	0.07	99
	5	Blue diamond	11784	<0.0001	0.15	101
	6	Dark green triangle	22047	<0.0006	0.24	45
	7	Dark red hexagon	22776	0.0556	0.13	19
	8	Dark blue square	4790	0.0055	0.13	29
	9	Dark cyan triangle	−7991	0.36	0.07	14
	10	Gray hexagon	2608	0.74	0.01	14
	11	Dark yellow triangle	45633	0.23	0.43	5
	12	Violet hexagon	39344	0.19	0.91	3
	13	Yellow square	8151	0.095	0.17	17
Bird 2						
	1	Black circle	1359	0.0088	0.11	63
	2	Cyan square	1040	0.163	0.05	39
	3	Red triangle	2085	<0.0001	0.78	137
	4	Light green hexagon	−4.9	0.978	0	111
	5	Blue diamond	297.9	0.0008	0.06	174
	6	Dark green triangle	−513.4	0.70	0.02	11
	7	Dark red circle	306.3	0.043	0.28	15
	8	Dark yellow square	1368	0.0059	0.68	9
	9	Gray triangle	814	<0.0001	0.18	159
	10	Pink hexagon	921	0.33	0.05	21
Bird 3						
	1	Black circle	−2.5	<0.0001	0.45	71
	2	Cyan square	1.42	0.0005	0.21	55
	3	Red triangle	−0.21	0.66	0.006	33
	4	Light green hexagon	−1.83	0.0526	0.13	29
	5	Blue diamond	−1.14	0.011	0.1	64
	6	Dark green square	0.44	0.6	0.008	34
	7	Dark red diamond	−0.53	0.61	0.006	43
	8	Dark green triangle	0.6	0.74	0.03	6

Within each file, syllables were characterized in terms of the initial frequency, final frequency, and syllabic rate. As for the synthetic data discussed before, we selected the times in which air sac pressure presented maxima. Then, we selected sound segments (1024 points) around those times, and we analyzed them spectrally. Finally, for each syllable type, we used linear regression analysis to describe the relationship between pressure and fundamental frequency. The results are summarized in Table I.

We analyzed 1555 syllables, corresponding to 31 syllable types, sung by three birds. We found that for high frequencies, there was a systematic positive slope in the relationship between the fundamental frequency and the peak air sac pressure, consistent with the signature of negative slopes of the isofrequency curves in that region of the parameter space. In bird number 1 [Fig. 4(a)], there was no syllable type presenting a fitting with a significant negative slope (5%). The same occurs for bird 2 [Fig. 4(b)], where the two syllable types with negative slope correspond to nonsignificant fittings. Bird 3 [Fig. 4(c)] does present two syllables with significant fittings with negative slopes, both of which are of low fundamental frequency.

Inspecting the isofrequencies in Fig. 1, we can see that for comparable frequencies the slopes can be different. For example, at 4 kHz, we find negative slopes for $\beta < 2$, while for larger values of β the slopes are near zero. The slopes can be positive for small values of the frequency if the values of β are large enough (that is the case for the isofrequency line corresponding to 2 kHz if $\beta > 0.5$). In terms of our data, one of the birds analyzed (bird 1) presented syllables at high frequency and low pressure values, as well as a syllable at a small frequency and high pressure, thus covering a wide range of slopes. This allows us to test the hypothesis that the slopes correlate positively with the average pressure. In Fig. 5, we display for bird 1 the slopes as a function of the average frequency. The values of the fitting are described in the caption.

For canaries, it has been suggested that sounds are generated as labia start to oscillate in a Hopf bifurcation. We have seen that a simple model of phonation with nonlinear dissipation and nonlinear restitution can be taken to a Hopf normal form. Its analysis allows us to characterize the isofrequency curves in the vicinity of the bifurcations, and, asymptotically close to the bifurcation, the slopes are negative. Notice that for finite values of the bifurcating parameter (β), for κ sufficiently low, the isofrequency slopes are positive, reflecting the relative importance of the nonlinear terms in the problem (see Fig. 1). Since negative (positive) slopes of the isofrequency curves

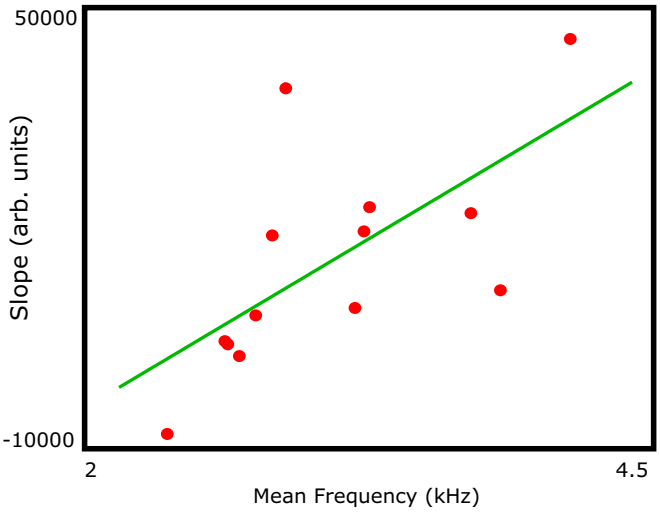

FIG. 5. (Color online) Positive correlation between *slope* and *average frequency* for vocalizations of Bird 1. Vertical axes display the slopes (*frequency*/*pressure*) from linear fit presented in Fig. 4(a) (see Table I for details). Horizontal axes: average fundamental frequency of the syllables. Each red dot corresponds to a particular syllable. The green line illustrates the linear regression. Fitting parameters: $f(x) = 18.42x - 41\,304.8$, $R^2 = 0.4319$.

imply positive (negative) slopes in the fittings of the frequency versus pressure plots, we conclude that our data from canaries are consistent with a nonlinear phonation mechanism in which a nonlinear restitution is present.

VI. CONCLUSIONS

In most animals that vocalize, fundamental frequency is an important acoustic feature for effective communication, and physiological regulation of sound frequency is therefore important for our understanding of vocal motor control. In the case of oscine birds, the activity of specific syringeal muscles [7,8] and the regulation of air sac pressure [9,10,24,25] play an intertwined role in frequency control. Dissecting the respective roles of each physiological parameter remains challenging, especially if one considers the remarkably diverse vocal repertoires of birds. In this work, we introduced the isofrequency curves in order to describe this synergistic interaction.

In a model containing both nonlinear dissipation and nonlinear restitution, each factor intervened in a specific manner, enriching the structure of the parameter space and the shapes of the isofrequency curves. The nonlinear restitution was found to be responsible for the negative slope of the isofrequency curves in the pressure-tension parameter space. This relationship was found to leave its fingerprint in the acoustic features of the syllables uttered by canaries.

How does this complex array of simultaneous activation patterns arise during vocal ontogeny? The parameter space might be systematically explored during the sensorimotor phase of song development, and, guided by acoustic feedback, birds may arrive at the effective activation patterns of all motor systems. The rapid dynamics of aerodynamic variables, as reflected in the shape of the expiratory pressure pulses, may provide the guiding trajectory in parameter space, which may in turn dictate the appropriate activation of the tension controlling syringeal muscles. At the conclusion of the sensorimotor phase, these effective patterns become stereotyped. However, small variation in respiratory and syringeal motor gestures between repetitions of the same syllable type generates variation in the behavioral output (i.e., sound frequency) [26].

The fact that frequency is allowed to vary according to the variation in air sac pressure and ventral syringeal muscle activity clearly shows that birds do not compensate fully (or perhaps not at all) for these small variations. This result has major implications for other research areas. First, it shows that for some syllables, singing more loudly results in an increase in sound frequency, whereas for others it can result in a decrease. Increasing sound amplitude is typically achieved by increased airflow, which is generated with increased subsyringeal pressure [27,28]. The various effects on sound frequency that result from increased air sac pressure indicate that this occurs naturally within a repeated sequence of syllables of a trill, and the same relationship can be expected for singing trills at different amplitude. Such increases in air sac pressure may occur in response to high levels of background noise (Lombard effect), and associated changes in sound frequency could, therefore, be a passive byproduct of singing more loudly rather than an adaptive change [28,29].

ACKNOWLEDGMENTS

This project was funded by NIH (RO1 DC-006876), CONICET, UBA, and ANCyT.

[1] S. A. Overduin, A. d'Avella, J. Roh, and E. Bizzi, J. Neurosci. **28**, 880 (2008).
[2] M. C. Tresch and A. Jarc, Curr. Opin. Neurobiol. **19**, 601 (2009).
[3] M. Haruno, D. M. Wolpert, and M. Kawato, Neural Comput. **13**, 2201 (2001).
[4] J. S. Kelso, B. Tuller, E. Vatikiotis-Bateson, and C. A. Fowler, J. Exp. Psychol. Hum. Percept. Perform. **10**, 812 (1984).
[5] T. Riede and F. Goller, Brain Language **115**, 69 (2010).
[6] F. Goller and T. Riede, J. Physiol. Paris **107**, 230 (2013).
[7] F. Goller and R. A. Suthers, J. Neurophysiol. **76**, 287 (1996).
[8] F. Goller, R. A. Suthers, J. Neurophysiol. **75**, 867 (1996).
[9] O. N. Larsen and F. Goller, J. Exp. Biol. **205**, 25 (2002).
[10] G. B. Mindlin, T. J. Gardner, F. Goller, and R. Suthers, Phys. Rev. E **68**, 041908 (2003).
[11] A. Amador, G. B. Mindlin, and F. Goller, J. Neurophysiol. **99**, 2383 (2008).
[12] T. Riede, J. H. Fisher, and F. Goller, PloS One **5**(6), e11368 (2010).

[13] J. D. Sitt, A. Amador, F. Goller, and G. B. Mindlin, Phys. Rev. E **78**, 011905 (2008).
[14] A. Amador and G. B. Mindlin, Chaos **18**, 043123 (2008).
[15] S. H. Strogatz, *Nonlinear Dynamics and Chaos: With Applications to Physics, Biology, Chemistry and Engineering* (Perseus, Cambridge, MA, 2001).
[16] I. R. Titze, J. Acoust. Soc. Am. **83**, 1536 (1988).
[17] C. P. Elemans, O. N. Larsen, M. R. Hoffmann, and J. L. van Leeuwen, Animal Biol.-Leiden **53**, 183 (2003).
[18] T. Gardner, G. Cecchi, M. Magnasco, R. Laje, and G. B. Mindlin, Phys. Rev. lett. **87**, 208101 (2001).
[19] A. Amador, Y. S. Perl, G. B. Mindlin, and D. Margoliash, Nature **495**, 59 (2013).
[20] R. Laje, T. J. Gardner, and G. B. Mindlin, Phys. Rev. E **65**, 051921 (2002).
[21] R. Laje and G. B. Mindlin, Phys. Rev. E **72**, 036218 (2005).
[22] J. C. Lucero and J. Schoentgen, Proceedings of Meetings on Acoustics **19**, 060165 (2013).
[23] M. A. Trevisan, G. B. Mindlin, and F. Goller, Phys. Rev. Lett. **96**, 058103 (2006).
[24] L. M. Alonso, J. A. Alliende, F. Goller, and G. B. Mindlin, Phys. Rev. E **79**, 041929 (2009).
[25] G. J. L. Beckers, R. A. Suthers, and C. ten Cate, J. Exp. Biol. **206**, 1833 (2003).
[26] A. Amador and D. Margoliash, J. Neurosci. **33**, 11136 (2013).
[27] E. M. Plummer and F. Goller, J. Exp. Biol. **211**, 66 (2008).
[28] H. Brumm and A. Zollinger, Behaviour **148**, 1173 (2011).
[29] S. A. Zollinger, J. Podos, E. Nemeth, F. Goller, and H. Brumm Animal Behaviour **84**, e1 (2012).